CrossMark

ORIGINAL PAPER

Vortex solitons of the (3+1)-dimensional spatially modulated cubic–quintic nonlinear Schrödinger equation with the transverse modulation

Rui-Pin Chen · Chao-Qing Dai

Abstract Vortex solitons in the spatially modulated cubic–quintic nonlinear media are governed by a (3+1)-dimensional cubic–quintic nonlinear Schrödinger equation with spatially modulated nonlinearity and transverse modulation. Via the variable separation principle with the similarity transformation, we derive two families of vortex soliton solutions in the spatially modulated cubic–quintic nonlinear media. For the disappearing and parabolic transverse modulation, vortex solitons with different configurations are constructed. The similar configurations of vortex solitons exist for the same value of $l - k$ with the topological charge k and degree number l. Moreover, the number of the inner layer structure of vortex solitons getting rid of the package covering layer is related to $(n - 1)/2 + 1$ with the soliton order number n. For the disappearing transverse modulation, there exist phase azimuthal jumps around their cores of vortex solitons with 2π phase change in every jump, and any two jumps one after another realize the change in π. For the parabolic transverse modulation, all phases of vortex soliton exist k-jump, and every jump realizes the change in $2\pi/k$; thus, k-jumps totally realize the azimuthal change in 2π around their cores.

1 Introduction

Over the past several decades, solitons based on the nonlinear Schrödinger equation (NLSE) exhibit widespread applications in various branches of physics, engineering and other disciplines [1–4]. Spatial and spatiotemporal solitons reveal different types of localized modes, including fundamental solitons [5,6], Peregrine solution and breather [7,8], multipole solitons [9,10] and vortex solitons [11,12], and so on.

Vortex solitons are optical beams which exist phase singularities mixed within the wave front curvature and carry a nonzero angular momentum, and extensively investigated in the context of optical tweezers [13], entanglement states of photons [14] and trapping and guiding of cold atoms [15]. In many kinds of media, such as Kerr, saturable-atomic and photorefractive nonlinear media, optical vortices have been studied experimentally and theoretically [16,17]. If a vortex generates an effective axisymmetric potential well, then this well may trap a bright two-dimensional solitary wave, producing some complex vector vortex solitons, such as the vortex-bright soliton [17], the half-quantum vortex [18] and the filled-core vortex [19].

In conservative nonlinear media, vortex solitons always lead to the symmetry breaking azimuthal insta-

R.-P. Chen (✉)
Department of Physics, Zhejiang Sci-Tech University, Hangzhou 310018, Zhejiang, People's Republic of China
e-mail: chenrp123@gmail.com

C.-Q. Dai
School of Sciences, Zhejiang A & F University, Lin'an 311300, Zhejiang, People's Republic of China

bility and collapse into many fundamental solitons. This instability can also be inhibited. In graded-index optical fibers [20], nonlinear photonic crystals with defects and optical lattices with defect [21], the confined potentials can suppress the azimuthal instability of vortices. Although vortex soliton in the (3+1)-dimensional case has been studied in Bose–Einstein condensates (BEC) [22], the influence of the transverse modulation on vortex soliton in the (3+1)-dimensional spatially modulated cubic–quintic (CQ) nonlinear media is relatively few studied.

As we all know, the CQ nonlinearities are considered when the optical field frequency is close to a resonant frequency of the optical fiber material in nonlinear optics [23,24]. On the other hand, in BEC with high density, the three-body interaction must be considered, and thus, the CQNLSE is used to describe this case [25]. After Serkin et al. firstly studied the topological quasi-soliton solutions of the variable coefficient CQNLSE [26], rich soliton modes of this equation have been derived [27,28]. Recently, soliton solutions in the media with CQ nonlinearities modulated in space and time have also been discussed [29–31]. However, these works studied solitons based on (1+1)-dimensional and (2+1)-dimensional cases [28–31], (3+1)-dimensional vortex solitons in the spatially modulated CQ nonlinear media with the transverse modulation have not been reported. In this paper, we focus on this case.

2 Model and exact vortex soliton solutions

In nonlinear fiber optics, a general (3+1)-dimensional NLSE is written as [35,36]

$$
\mathrm{i}\frac{\partial A}{\partial z} + \frac{1}{2\beta_0}\left(\frac{\partial^2 A}{\partial x^2} + \frac{\partial^2 A}{\partial y^2}\right) + \frac{\beta_2}{2}\frac{\partial^2 A}{\partial t^2} + \gamma |A|^2 A = 0,
\tag{1}
$$

where the pulse envelope $A = A(z, x, y, t)$, the dispersion parameter β_2 can be positive or negative with magnitude of the order of $10^{-3} - 10^{-2}\mathrm{ps}^2/\mathrm{m}$ [35] and the propagation parameter $\beta_0 = 2\pi n_0/\lambda$ with the refractive index n_0 and the wave length of the beam λ [36]. The unit of the nonlinear parameter γ and $|A|^2$ is $W^{-1}\mathrm{m}$ and $W\mathrm{m}^{-2}$, respectively. By scaling, we define the following dimensionless variables $x = x/\rho, y = y/\rho, t = t/\tau, z = z/L_\mathrm{D}, \phi =$

$A\rho/\sqrt{P_0}, p = \gamma P_0 L_\mathrm{D}/\rho^2$ [35] with lengths for dispersion or diffraction ($L_\mathrm{DS} = L_\mathrm{DF} = L_\mathrm{D}$), the radius of the beam ρ, the timescale of the soliton τ, power P_0, Eq. (1) can be transformed into the dimensionless form. Considering CQ nonlinearities, we obtain the following dimensionless NLS equations with self-focusing cubic and self-defocusing quintic nonlinearity [36,37]

$$
\mathrm{i}\frac{\partial \phi}{\partial z} + \frac{1}{2}\left(\frac{\partial^2 \phi}{\partial x^2} + \frac{\partial^2 \phi}{\partial y^2} + \frac{\partial^2 \phi}{\partial t^2}\right) + p|\phi|^2\phi - q|\phi|^4\phi = 0,
\tag{2}
$$

where $\phi = \phi(z, x, y, t)$.

Recently, spatially modulated nonlinearity and transverse modulation are introduced to study the dynamics of solitons [29–31], and thus, the (3+1)-dimensional CQNLSE with spatially modulated nonlinearity and transverse modulation reads

$$
\mathrm{i}\frac{\partial \phi}{\partial z} + \frac{1}{2}\left(\frac{\partial^2 \phi}{\partial x^2} + \frac{\partial^2 \phi}{\partial y^2} + \frac{\partial^2 \phi}{\partial t^2}\right)
$$
$$
+ \chi_3(r)|\phi|^2\phi + \chi_5(r)|\phi|^4\phi + R(r)\phi = 0,
\tag{3}
$$

where the cubic nonlinearity coefficient $\chi_3(r)$, quintic nonlinearity coefficient $\chi_5(r)$ and the transverse modulation $R(r)$ are all functions of radial coordinate $r \equiv (x, y, t)$. In BEC, ϕ represents the macroscopic wave function of the condensate with time z, $R(r)$ is the external potential. In this paper, we choose parabolic transverse modulation or external potential. Other external potentials can be found in Refs. [32–34].

In the following, we use dimensionless form and units to calculate, and these results can be easily converted to actual experimental units following the guidelines by considering some similar values in an experiment on spatiotemporal soliton in a planar glass waveguide, namely wave length $\lambda = 1\,\mu\mathrm{m}$, $\beta_2 = 10^{-2}\mathrm{ps}^2/\mathrm{m}$, and the timescale $\tau = 60$ fs; thus, the propagation length $L_\mathrm{D} = 36$ cm and the beam width $\rho \approx 239\,\mu\mathrm{m}$.

We assume that Eq. (3) has the spatially localized vortex soliton solution in the form

$$
\phi(r, \theta, \varphi, z) = \rho(r)\psi(\theta, \varphi)\exp(-\mathrm{i}\sigma z),
\tag{4}
$$

where σ is the propagation constant in optics and the chemical potential in BEC, and the real function $\rho(r)$ satisfies the localization condition $\lim_{r\to\pm\infty}\rho(r) = 0$.

Substituting Eq. (4) into Eq. (3), and considering $\psi(\theta, \varphi) = \sqrt{\frac{(2l+1)(l-k)!}{2\pi(l+k)!}} \times P_l^k(\cos\theta)\exp(ik\varphi)$ where the topological charge k and the associated Legendre polynomials $P_l^k(\cos\theta)$ with the degree l and order k satisfying $l \geq k \geq 0$, one obtains

$$\frac{r^2}{\rho} \left\{ \frac{1}{r^2} \frac{\partial}{\partial r}(r^2 \frac{\partial\rho}{\partial r}) + 2[\sigma + R(r)]\rho \right.$$
$$\left. + 2\chi_3(r)\rho^3 + 2\chi_5(r)\rho^4 \right\} = l(l+1), \quad (5)$$

Following the scheme proposed in Refs. [28–31], if we assume $\rho(r) \equiv \varrho(r)\Psi[\zeta(r)]$ where $\Psi(\zeta)$ satisfying

$$\frac{d^2\Psi}{d\zeta^2} + G_1\Psi + G_3\Psi^3 + G_5\Psi^5 = 0, \quad (6)$$

with three constants G_1, G_3 and G_5 and consider $\zeta(r) \equiv \int_0^r \varrho^{-2}(s)s^{-1}ds$, then Eq. (5) transforms into

$$\varrho'' + \frac{2}{r}\varrho' + \left[2\sigma + 2R(r) - \frac{l(l+1)}{r^2}\right]\varrho = \frac{G_1}{r^4\varrho^3}, \quad (7)$$

and nonlinear functions $\chi_3(r)$ and $\chi_5(r)$ satisfy $\chi_3(r) = G_3 r^{-2}\varrho^{-6}(r)/2$, $\chi_5(r) = G_5 r^{-2}\varrho^{-8}(r)/2$.

If we choose $\varrho(r) = \eta(r)/r$, then Eq. (7) changes into the Ermakov–Pinney equation as $\eta_{rr} + [2\sigma + 2R(r) - l(l+1)/r^2]\eta = G_1/\eta^3$ [38]. If G_1 is a constant, then $\eta(r)$ can be expressed as $\eta = \sqrt{\alpha\xi_1^2 + 2\beta\xi_1\xi_2 + \gamma\xi_2^2}$ where $G_1 = (\alpha\gamma - \beta^2)W^2$ with three constants α, β, γ and Wronskian $W = \xi_1\xi_{2r} - \xi_2\xi_{1r} = $ constant with $\xi_1(r)$ and $\xi_2(r)$ being two linearly independent solutions of $\xi_{rr} + [2\sigma + 2R(r) - l(l+1)/r^2]\xi = 0$. Further, if $G_1 = 0$ and $R(r)$ is the parabolic transverse modulation with $R(r) = \frac{1}{2}\omega^2 r^2$, then $\varrho(r) = r^{-\frac{3}{2}}[c_1 M(\frac{\sigma}{2\omega}, \frac{l}{2} + \frac{1}{4}, \omega r^2) + c_2 U(\frac{\sigma}{2\omega}, \frac{l}{2} + \frac{1}{4}, \omega r^2)]$ with the Whittaker's M and U functions [39], and constants $c_1 c_2 > 0$. Without considering the transverse modulation with $R(r) = 0$, $\varrho(r) = r^{-\frac{1}{2}}[c_3 J(l + 1/2, \sqrt{2\sigma}r) + c_4 Y(l + 1/2, \sqrt{2\sigma}r)]$ with the Bessel functions of the first kind J and second kind Y, and constants $c_3 c_4 > 0$.

Using a one-to-one correspondence between Eq. (3) and Eq. (6) with $G_1 = 0$, $G_3 = \frac{2}{3}\mu n^2 K^2(m)(m^4 - m^2 + 1)$, $G_5 = \frac{1}{9}\mu^2 n^2 K^2(m)(m^2 - 2)(2m^2 - 1)(m^2 +$

1), we obtain two families of exact vortex soliton solutions for Eq. (3) as

$$\phi_{1n} = \sqrt{\frac{(2l+1)(l-k)!}{2\pi(l+k)!}} P_l^k$$
$$(\cos\theta)\frac{3\varrho(r)\text{sn}[\lambda K(m), m]}{\sqrt{3\mu[3 - (m^2+1)\text{sn}^2[\lambda K(m), m]]}}e^{ik\varphi - i\sigma z}, \quad (8)$$

with $\lambda = n\zeta + 1$ for $n = 1, 3, 5, \ldots$, while for $n = 2, 4, 6, \ldots$,

$$\phi_{2n} = \sqrt{\frac{(2l+1)(l-k)!}{2\pi(l+k)!}} P_l^k$$
$$(\cos\theta)\frac{3\varrho(r)\text{sn}[nK(m)\zeta, m]}{\sqrt{3\mu[3 - (m^2+1)\text{sn}^2[nK(m)\zeta, m]]}}e^{ik\varphi - i\sigma z}, \quad (9)$$

where μ is a real constant, the integer n is associated with the soliton order number, sn is the Jacobian elliptic sine function with the modulus m and $K(m) = \int_0^{\pi/2}[1 - m^2\sin^2(\xi)]^{-1/2}d\xi$ is elliptic integral of the first kind [40].

3 Construction of vortex solitons

Solutions (8) and (9) describe vortex solitons with different configurations. For the disappearing transverse modulation $R = 0$, vortex solitons of solutions (8) and (9) with different values of k and l are shown in Fig. 1. When $k = l = 0$, localized spheres of solutions (8) and (9) are displayed in Fig. 1a, b, respectively. When $k = 0, l = 1$, solution (9) describes a cylinder as shown in Fig. 1d, and solution (8) describes a sphere surrounded by a cylinder as shown in Fig. 1c. When $k = l = 1$, two discs with symmetrical distribution on two sides of the plane $t = 0$ are constructed in Fig. 1f, and two symmetrical spheres surrounded by two discs are constructed in Fig. 1e. In Fig. 1g for solution (8) with $k = 0, l = 2$, a pair of drip-shaped structures embed above and below the torus-shaped structure in the middle, and the whole structure is surrounded by a cylinder, which also appears in Fig. 1h for solution (9). When $k = 1, l = 2$, two cones with symmetrical distribution on two sides of the plane $t = 0$ are constructed in Fig. 1j, and two symmetrical toruses surrounded by two cones are constructed in Fig. 1i. When $k = l = 2$, structures in Fig. 1k, l are similar to those in Fig. 1e, f, and the difference is that the distance between two discs adds. In Fig. 1m for solution (8) with $k = 1, l = 3$, a
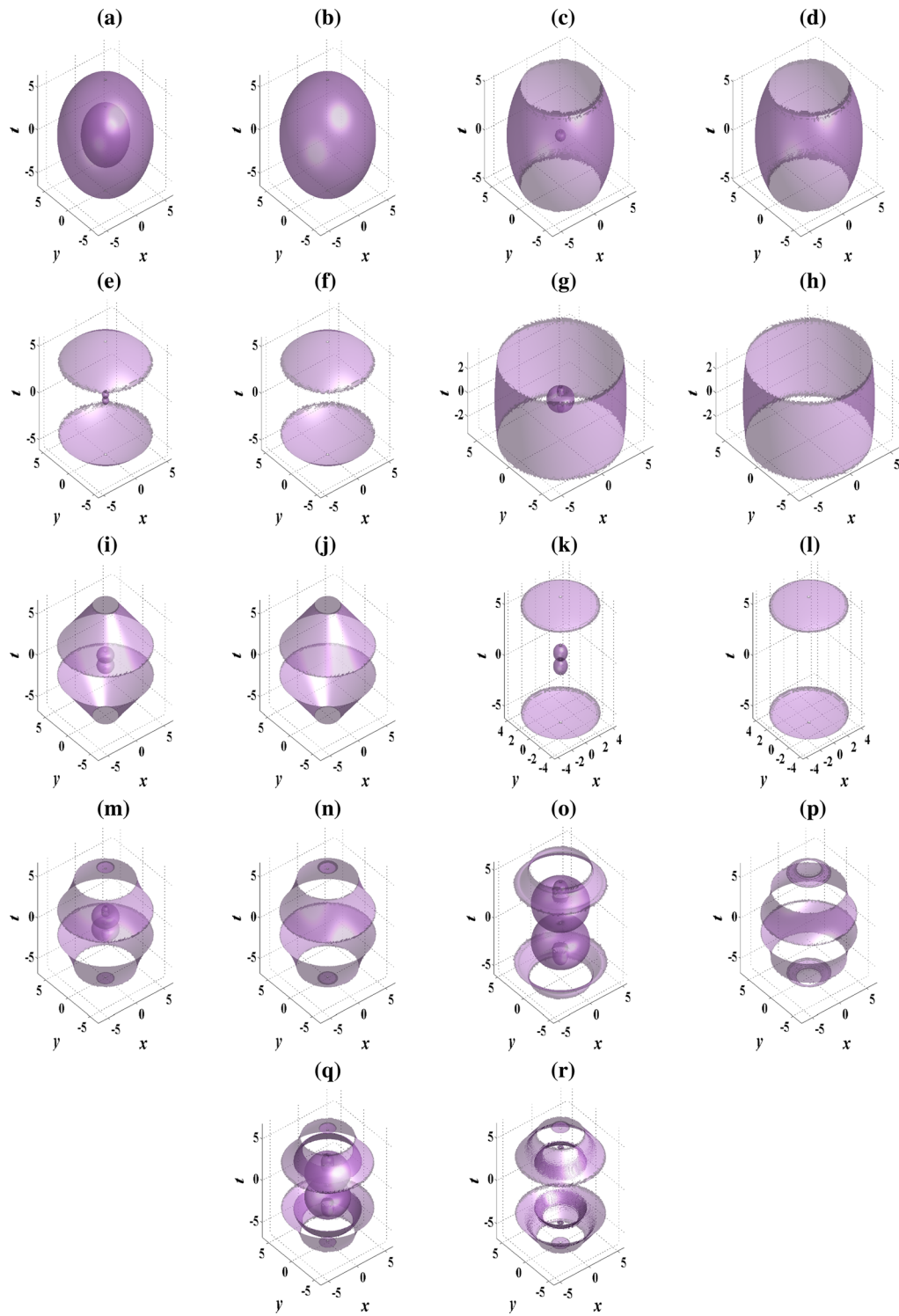
Fig. 1 (Color online) Vortex solitons with (**a**, **c**, **e**, **g**, **i**, **k**, **m**, **o**, **q**) solution (8) and (**b**, **d**, **f**, **h**, **j**, **l**, **n**, **p**, **r**) solution (9) for the disappearing transverse modulation $R = 0$. The parameters are chosen as $\sigma = 0.3$, $\mu = 0.1$, $m = 0.1$, $c_3 = 1$, $c_4 = 1.5$, $n = 1$ with **a**, **b** $k = l = 0$; **c**, **d** $k = 0, l = 1$; **e**, **f** $k = l = 1$; **g**, **h** $k = 0, l = 2$; **i**, **j** $k = 1, l = 2$; **k**, **l** $k = l = 2$; **m**, **n** $k = 1, l = 3$; **o**, **p** $k = 2, l = 4$ and **q**, **r** $k = 3, l = 5$
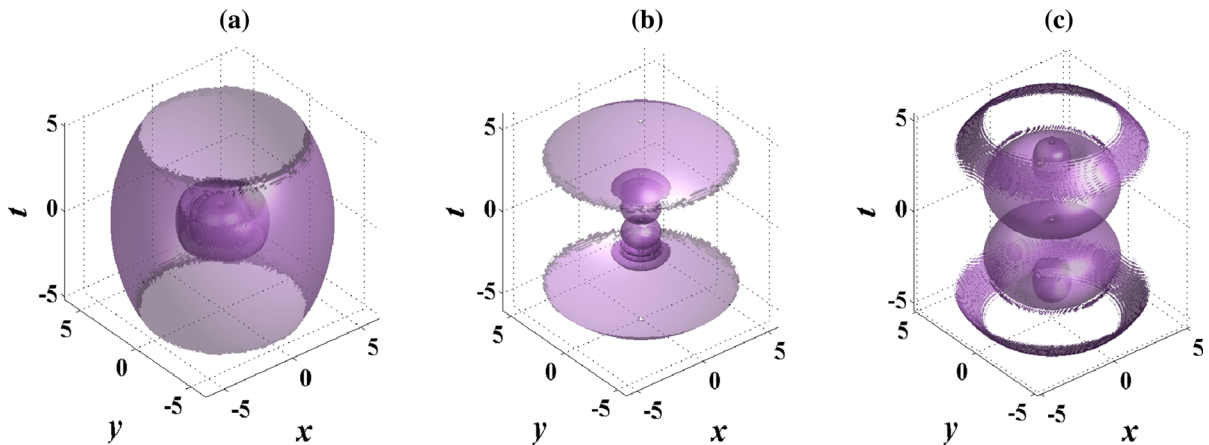
Fig. 2 (Color online) Vortex solitons with solution (8) for the disappearing transverse modulation $R = 0$. The parameters are chosen as those in Fig. 1 except for **a** $k = 0, l = 1, n = 3$, **b** $k = l = 1, n = 7$ and **c** $k = 2, l = 4, n = 3$

pair of drip-shaped structures also appear above and below the pair of torus-shaped structures in the middle, and the whole structure is surrounded by two cones, where every cone is closed by a disc at the end. These cones also are shown in Fig. 1n for solution (9). When $k = 2, l = 4$, structures in Fig. 1o, p are similar to those in Fig. 1m, n, and the difference is that all parts of structures enlarge. When $k = 3, l = 5$, two nested structures with the arranges of two cones closed by a disc at the end one by one distribute symmetrically on two sides of the plane $t = 0$ in Fig. 1r, and inside the whole structure in Fig. 1r, a pair of drip-shaped structures also exist above and below the pair of torus-shaped structures in the middle in Fig. 1q. From these structures in Fig. 1e, f, k, l, and Fig. 1m–p, we find that similar structures can be constructed for the same value of $l - k$.

Figure 2 displays multi-layer structures of vortex solitons for $n = 3, 7$. Compared Fig. 1c for $n = 1$ with Fig. 2a for $n = 3$ and Fig. 1o for $n = 1$ with Fig. 2c for $n = 3$, there is an extra layer structure in both structures for $n = 3$. Compared Fig. 1e for $n = 1$ with Fig. 2b for $n = 7$, there are three extra layers in the structure for $n = 7$. Therefore, the number of the inner layer structure getting rid of the package covering layer is related to $(n - 1)/2 + 1$ with the soliton order number n.

Figure 3 shows phases of vortex solitons with solutions (8) and (9) for the disappearing transverse modulation $R = 0$ at $t = 0$ when k, l, n are chosen as different values. All phases of vortex solitons in Fig. 3

exist an azimuthal jump around their cores with different values of k, l, n. In Fig. 3a, there exist two azimuthal jumps, and every jump realizes the change in 2π; however, the phase change from the first jump to second jump is π. In Fig. 3b, there exist three azimuthal jumps with 2π phase change in every jump, and two jumps one after another realize the change in π; thus, two changes totally produce the change in 2π. In Fig. 3c, there exist six jumps, that is, five change in two jumps one after another, and thus, totally produces the change in 5π. Similar analysis for Figs. 3d–i can be used, and we omit it for the limit of length.

In the presence of the parabolic transverse modulation $R = \varpi^2 r^2/2$, vortex solitons can be also constructed. Figure 4 presents some cases of vortex solitons with the intensity and corresponding phases. When $k = 0, l = 1$, solution (9) with $n = 1$ describes a cylinder with bell mouthed shape in Fig. 4b, and solution (8) with $n = 2$ describes a torus-shaped structure surrounded by a cylinder with bell mouthed shape in Fig. 4a. When $k = l = 1$, two trays with symmetrical distribution on two sides of the plane $t = 0$ are constructed in Fig. 4d, and two symmetrical flattened ellipsoids surrounded by two trays are constructed in Fig. 4c. From the phase plot in Fig. 4e, when $m = l = 1$, it is similar to the case for the disappearing transverse modulation $R = 0$, that is, there exist two azimuthal jumps with 2π phase change in every jump, and two jumps one after another realize the change in π. However, when $k = l = 2, 3, 4$, the phase change in vortex soliton in presence of the parabolic transverse

(a)

(b)

(c)

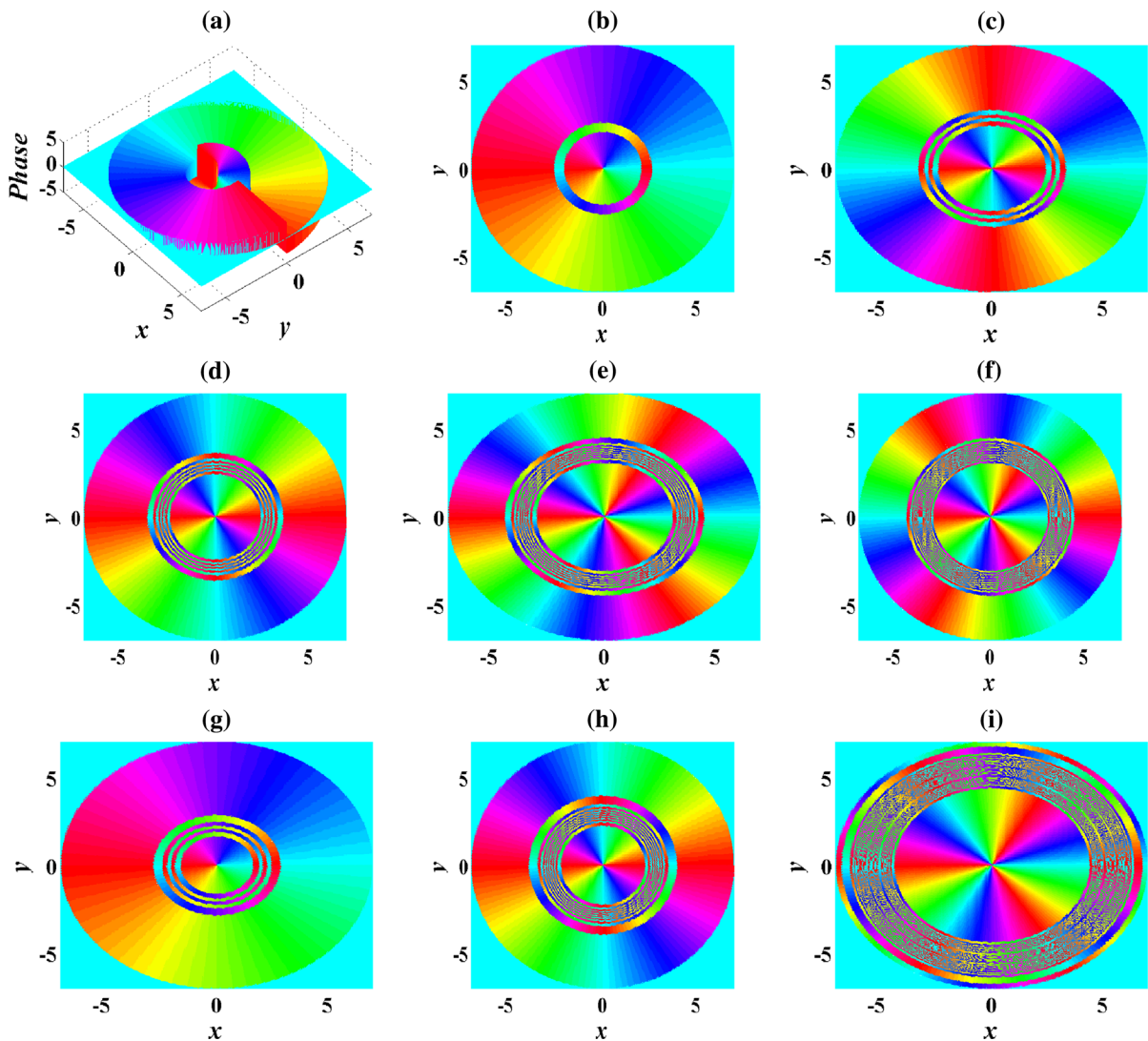**(d)**

(e)

(f)

(g)

(h)

(i)

Fig. 3 (Color online) Phases of vortex solitons with solutions (8) and (9) for the disappearing transverse modulation $R = 0$ at $t = 0$. The parameters are chosen as those in Fig. 1 except for **a** $k = l = 1, n = 1$, **b** $k = l = 1, n = 2$, **c** $k = l = 2, n = 1$, **d** $k = l = 2, n = 2$, **e** $k = l = 3, n = 1$, **f** $k = l = 3, n = 2$, **g** $k = l = 1, n = 5$, **h** $k = l = 2, n = 3$ and **i** $k = 3, l = 5, n = 3$

modulation $R = \varpi^2 r^2/2$ is different from those for the disappearing transverse modulation $R = 0$. From Fig. 4f–h, all phases of vortex soliton exist k-jump with different values of the topological charge k, and every jump realizes the change in $2\pi/k$; thus, k-jumps totally realize the azimuthal change in 2π around their cores.

4 Conclusion

In conclusion, with the help of the variable separation principle with the similarity transformation, we derive

two families of vortex soliton solution in the spatially modulated CQ nonlinear media governed by a (3+1)-dimensional CQNLSE with spatially modulated nonlinearity and transverse modulation. For the disappearing and parabolic transverse modulations, vortex solitons with different configurations are constructed. The similar configurations of vortex solitons exist for the same value of $l - k$ with the topological charge k and degree number l. Moreover, the number of the inner layer structure of vortex solitons getting rid of the pack-
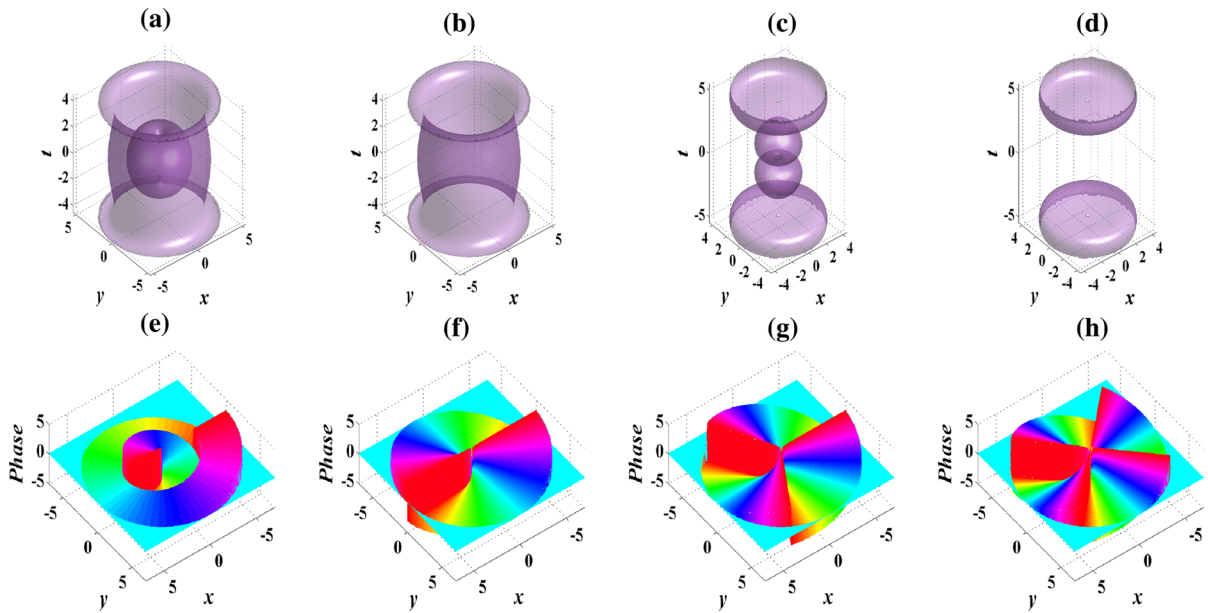
Fig. 4 (Color online) **a**–**d** Intensity and **e**–**f** phase of vortex solitons in the presence of the parabolic transverse modulation $R = \omega^2 r^2/2$. The parameters are chosen as those in Fig. 1 except for $\omega = 0.01$ with **a** $k = 0, l = 1, n = 1$, **b** $k = 0, l = 1, n = 2$, **c**, **e** $k = l = 1, n = 1$; **d** $k = l = 1, n = 2$, **f** $k = l = 2, n = 1$, **g** $k = l = 3, n = 1$ and **h** $k = l = 4, n = 1$

age covering layer is related to $(n-1)/2+1$ with the soliton order number n. For the disappearing transverse modulation, there exist phase azimuthal jumps around their cores of vortex solitons with 2π phase change in every jump, and any two jumps one after another realize the change in π. For the parabolic transverse modulation, all phases of vortex solitons exist k-jump with different values of the topological charge k, and every jump realizes the change in $2\pi/k$; thus, k-jumps totally realize the azimuthal change in 2π around their cores.

References

1. Kong, L.Q., Liu, J., Jin, D.Q., Ding, D.J., Dai, C.Q.: Soliton dynamics in the three-spine α-helical protein with inhomogeneous effect. Nonlinear Dyn. **87**, 83–92 (2017)

2. Serkin, V.N., Hasegawa, A., Belyaeva, T.L.: Nonautonomous solitons in external potentials. Phys. Rev. Lett. **98**, 074102 (2007)

3. Li, J.T., Zhu, Y., Liu, Q.T., Han, J.Z., Wang, Y.Y., Dai, C.Q.: Vector combined and crossing Kuznetsov–Ma solitons in PT-symmetric coupled waveguides. Nonlinear Dyn. **85**, 973–980 (2016)

4. Kong, L.Q., Dai, C.Q.: Some discussions about variable separation of nonlinear models using Riccati equation expansion method. Nonlinear Dyn. **81**, 1553–1561 (2015)

5. Dai, C.Q., Fan, Y., Zhou, G.Q., Zheng, J., Cheng, L.: Vector spatiotemporal localized structures in (3 + 1)-dimensional strongly nonlocal nonlinear media. Nonlinear Dyn. **86**, 999–1005 (2016)

6. Dai, C.Q., Chen, R.P., Wang, Y.Y., Fan, Y.: Dynamics of light bullets in inhomogeneous cubic-quintic-septimal nonlinear media with PT-symmetric potentials. Nonlinear Dyn. **87**, 1675–1683 (2017)

7. Wang, Y.Y., Dai, C.Q., Zhou, G.Q., Fan, Y., Chen, L.: Rogue wave and combined breather with repeatedly excited behaviors in the dispersion/diffraction decreasing medium. Nonlinear Dyn. **87**, 67–73 (2017)

8. Dai, C.Q., Liu, J., Fan, Y., Yu, D.G.: Two-dimensional localized Peregrine solution and breather excited in a variable-coefficient nonlinear Schrödinger equation with partial nonlocality. Nonlinear Dyn. **88**, 1373–1383 (2017)

9. Xu, Y.J.: Hollow ring-like soliton and dipole soliton in (2+1)-dimensional PT-symmetric nonlinear couplers with gain and loss. Nonlinear Dyn. **83**, 1497–1501 (2016)

10. Wu, H.Y., Jiang, L.H.: Vector Hermite–Gaussian spatial solitons in (2+1)-dimensional strongly nonlocal nonlinear media. Nonlinear Dyn. **83**, 713–718 (2016)

11. Zhu, H.P., Pan, Z.H.: Vortex soliton in (2+1)-dimensional PT-symmetric nonlinear couplers with gain and loss. Nonlinear Dyn. **83**, 1325–1330 (2016)

12. Zhu, H.P., Chen, L., Chen, H.Y.: Hermite–Gaussian vortex solitons of a (3+1)-dimensional partially nonlocal nonlinear Schrodinger equation with variable coefficients. Nonlinear Dyn. **85**, 1913–1918 (2016)

13. Paterson, L., MacDonald, M.P., Arlt, J., Sibbett, W., Bryant, P.E., Dholakia, K.: Controlled rotation of optically trapped microscopic particles. Science **292**, 912–914 (2001)

14. Mair, A., Vaziri, A., Weihs, G., Zeilinger, A.: Entangled singularity patterns of photons in Ince-Gauss modes. Nature **412**, 313–316 (2001)

15. Kuga, T., Torii, Y., Shiokawa, N., Hirano, T., Shimizu, Y., Sasada, H.: Novel optical trap of atoms with a doughnut beam. Phys. Rev. Lett. **78**, 4713–4716 (1997)

16. Wu, L., Li, L., Zhang, J.F.: Controllable generation and propagation of asymptotic parabolic optical waves in graded-index waveguide amplifiers. Phys. Rev. A **78**, 013838 (2008)

17. Law, K.J.H., Kevrekidis, P.G., Tuckerman, L.S.: Stable Vortex–Bright-soliton structures in two-component Bose–Einstein condensates. Phys. Rev. Lett. **105**, 160405 (2010)

18. Eto, M., Kasamatsu, K., Nitta, M., Takeuchi, H., Tsubota, M.: Short-range intervortex interaction and interacting dynamics of half-quantized vortices in two-component Bose–Einstein condensates. Phys. Rev. A **83**, 063603 (2011)

19. Anderson, B.P., Haljan, P.C., Wieman, C.E., Cornell, E.A.: Vortex precession in Bose–Einstein condensates: observations with filled and empty cores. Phys. Rev. Lett. **85**, 2857 (2000)

20. Abad, M., Guilleumas, M., Mayol, R., Pi, M.: Dipolar condensates confined in a toroidal trap: ground state and vortices. Phys. Rev. A **81**, 043619 (2010)

21. Dong, L.W., Li, H.J., Huang, C.M., Zhong, S.S., Li, C.Y.: Higher-charged vortices in mixed linear-nonlinear circular arrays. Phys. Rev. A **84**, 043830 (2011)

22. Lashkin, V.M.: Stable three-dimensional spatially modulated vortex solitons in Bose–Einstein condensates. Phys. Rev. A **78**, 033603 (2008)

23. Pusharov, D.I., Tanev, S.: Bright and dark solitary wave propagation and bistability in the anomalous dispersion region of optical waveguides with third- and fifth-order nonlinearities. Opt. Commun. **124**, 354–364 (1996)

24. Mani Rajan, M.S.: Unexpected behavior on nonlinear tunneling of chirped ultrashort soliton pulse in non-kerr media with Raman effect. Z. Naturforsch. A **71**, 751–758 (2016)

25. Abdullaev, F.K., Salerno, M.: Gap-Townes solitons and localized excitations in low-dimensional Bose–Einstein condensates in optical lattices. Phys. Rev. A **72**, 033617 (2005)

26. Serkin, V.N., Belyaeva, T.L., Alexandrov, I.V., Melchor, G.M.: Novel topological quasi-soliton solutions for the non-linear cubic–quintic Schrodinger equation model. Proce. SPIE Int. Soc. Opt. Eng. **4271**, 292–302 (2001)

27. Dai, C.Q., Chen, R.P., Wang, Y.Y.: Spatiotemporal self-similar solutions for the nonautonomous (3+1)-dimensional cubic–quintic Gross–Pitaevskii equation. Chin. Phys. B **21**, 030508 (2012)

28. Dai, C.Q., Wang, D.S., Wang, L.L.: Quasi-two-dimensional Bose–Einstein condensates with spatially modulated cubic–quintic nonlinearities. Ann. Phys. **326**, 2356–2368 (2011)

29. Belmonte-Beitia, J., Cuevas, J.: Solitons for the cubic–quintic nonlinear Schrodinger equation with time- and space-modulated coefficients. J. Phys. A Math. Theor. **42**, 165201 (2009)

30. Avelar, A.T., Bazeia, D., Cardoso, W.B.: Solitons with cubic and quintic nonlinearities modulated in space and time. Phys. Rev. E **79**, 025602 (2009)

31. Song, X., Li, H.M.: Stable vortex solitons of (2 + 1)-dimensional cubic–quintic Gross–Pitaevskii equation with spatially inhomogeneous nonlinearities. Phys. Lett. A **377**, 714–717 (2013)

32. Mahalingam, A., Mani Rajan, M.S.: Influence of generalized external potentials on nonlinear tunneling of nonautonomous solitons: soliton management. Opt. Fiber Tech. **25**, 44–50 (2015)

33. Mani Rajan, M.S., Mahalingam, A.: Multi-soliton propagation in a generalized inhomogeneous nonlinear Schrodinger–Maxwell–Bloch system with loss/gain. J. Math. Phys. **54**, 043514 (2013)

34. Dai, C.Q., Zhou, G.Q., Wang, X.G.: Stable light-bullet solutions in the harmonic and parity-time-symmetric potentials. Phys. Rev. A **89**, 013834 (2014)

35. Agrawal, G.P.: Nonlinear fiber optics: its history and recent progress. J. Opt. Soc. Am. B **28**, A1–A10 (2011)

36. Kivshar, Y.S., Agrawal, G.: Optical Solitons: From Fibers to Photonic Crystals. Academic Press, San Diego (2003)

37. Adhikari, S.K.: Elastic collision and molecule formation of spatiotemporal light bullets in a cubic–quintic nonlinear medium. Phys. Rev. E **94**, 032217 (2016)

38. Belmonte-Beitia, J., Perez-Garcia, V.M., Vekslerchik, V., Torres, P.J.: Lie symmetries and solitons in nonlinear systems with spatially inhomogeneous nonlinearities. Phys. Rev. Lett. **98**, 064102 (2007)

39. Whittaker, E.T., Watson, G.N.: A Course in Modern Analysis, 4th edn. Cambridge University Press, Cambridge (1990)

40. Abramowitz, M., Stegun, I.: Handbook of Mathematical Functions. Dover, New York (1965)